International Journal of Pharmaceutics 402 (2010) 238–247

Contents lists available at ScienceDirect

International Journal of Pharmaceutics

journal homepage: www.elsevier.com/locate/ijpharm

Pharmaceutical Nanotechnology

Enhanced anti-glioblastoma efficacy by PTX-loaded PEGylated poly(ε-caprolactone) nanoparticles: In vitro and in vivo evaluation

Hongliang Xin, Liangcen Chen, Jijin Gu, Xiaoqing Ren, Zhang wei, Jieqi Luo, Yanzuo Chen, Xinyi Jiang, Xianyi Sha, Xiaoling Fang*

Department of Pharmaceutics, School of Pharmacy, Fudan University, Lane 826,Zhangheng Road, Shanghai 201203, China

ARTICLE INFO

Article history:
Received 10 July 2010
Received in revised form
30 September 2010
Accepted 3 October 2010
Available online 8 October 2010

Keywords:
Polymeric nanoparticles
MPEGylated poly(ε-caprolactone)
Paclitaxel
Glioblastoma

ABSTRACT

The aim of this work was to investigate the anti-tumor effect of paclitaxel (PTX)-loaded methoxy poly(ethylene glycol)-poly(ε-caprolactone) nanoparticles (MPEG-NP/PTX) against glioblastoma multiforme (GBM). MPEG-NP/PTX was prepared by the emulsion and evaporation technique with particle size of 72.5 ± 2.2 nm and did not change remarkably during the period of 21-day storage at 4 °C. The drug-loading coefficient and encapsulation ratio of optimized formulation were 8.2 ± 0.6% and 90.4 ± 2.3%, respectively. The in vitro release behavior exhibits a biphase release manner and was affected by PEG segment. In vitro cytotoxicity was assessed using C6 cell lines and was compared to Taxol and PTX-loaded poly(ε-caprolactone) conventional nanoparticles (NP/PTX). Cell viability assay against C6 cells exhibited higher or at least comparable cytotoxicity than that of Taxol and NP/PTX. More importantly, in vivo real-time fluorescence imaging analysis in intracranial C6 glioblastoma bearing mice showed that the methoxy poly(ethylene glycol)-poly(ε-caprolactone) nanoparticles (MPEG-NP) displayed much stronger fluorescence signal and 3-fold larger Area-Under-Curve (AUC) than poly(ε-caprolactone) conventional nanoparticles (NP) in tumor-bearing brain. Furthermore, in vivo anti-glioblastoma effect exhibited the mean survive time of MPEG-NP/PTX (28 days) was much longer than those of Taxol injection (20 days) and NP/PTX (23 days). Therefore, MPEGylated poly(ε-caprolactone) nanoparticles significantly enhanced the anti-glioblastoma activity of PTX and might be considered a promising drug delivery system against advanced glioblastoma.

1. Introduction

Glioblastoma multiforme (GBM) is the most frequent primary central nervous system tumor, which represents the second cause of cancer death in adults less than 35 years of age (Allard et al., 2009). Since GBM differs from the other cancers by its diffuse invasion of the surrounding normal tissue, it is impossible to make the complete removal of tumor by the conventional surgical method and tumor recurrence from residual tumors is very possible (Ong et al., 2009). Consequently, it is critical to deliver the therapeutic agent effectively to the tumor as well as to infiltrate cells that are not located in the tumor bed for GBM treatment.

Paclitaxel (PTX), one of the most successful anticancer drugs, is the first of a new class of microtubule stabilizing agents and has demonstrable antitumor activity in glioma cell lines and animal model system of brain tumor (Régina et al., 2008; Desai et al., 2008; Heimans et al., 1994). However, because of the poor aqueous solubility and low therapeutic index of PTX, the clinical application is extremely limited. One commercial preparation of PTX is Taxol, a concentrated solution composed of a 50:50 (v/v) mixture of Cremophor EL (polyoxyl 35 castor oil) and dehydrated alcohol, which is diluted 5–20 fold in normal saline or dextrose solution before administration. Unfortunately, this vehicle is associated with serious side effects, such as hypersensitivity, nephrotoxicity and neurotoxicity as well as effects on endothelial and vascular muscles, causing vasodilatation, labored breathing, lethargy and hypotension (Weiss et al., 1990), and may interfere with taxane pharmacokinetics and antitumor activity (Ten tije et al., 2003). Furthermore, it is reported that the activity of PTX against brain tumor has been disappointing in a phase II study because of drug-resistant and poor penetration across the blood–brain barrier (BBB) (Chang et al., 2001; Postma et al., 2000).

Thereafter, alternative formulations that possess solubilization instead of Cremophor EL/alcohol as well as penetration across the BBB should be developed. With this in mind, colloidal drug carriers such as polymeric nanoparticles merit attention. However, as for the conventional polymeric nanoparticles, their rapid clearance from blood circulation by tissues of the Mononuclear Phagocyte System (MPS) is the major obstacle to deliver the active agent to the targeted sites such as tumor. Based on the modifications

* Corresponding author. Tel.: +86 21 51980071; fax: +86 21 51980072.
E-mail address: xlfang@shmu.edu.cn (X. Fang).

0378-5173/$ – see front matter © 2010 Elsevier B.V. All rights reserved.
doi:10.1016/j.ijpharm.2010.10.005

through physical adsorption of a hydrophilic polymer or synthesis of amphiphilic copolymer, long-circulating nanoparticles are testified for drug delivery to brain. Poly(butylcyanoacrilate) (PBCA) nanoparticles loaded with dalargin (Kreuter et al., 1997), loperamide (Alyautdin et al., 1997), doxorubicin (Ambruosi et al., 2005, 2006; Steiniger et al., 2004; Gulyaev et al., 1999), and NMDA-receptor antagonists (Friese et al., 2000) coated with a surfactant such as polysorbate 80 were shown to be able to cross BBB when administered intravenously. A number of studies showed that MPEGylated polycyanoacrilate nanoparticles penetrated into the brain to a larger extent than polysorbate 80 coated nanoparticles and conventional non-MPEGylated polycyanoacrilate nanoparticles (Calvo et al., 2001, 2002). Unfortunately, the cyanoacrilate-based polymers for human use have not been approved by U.S. Food and Drug Administration (FDA) yet, and its toxicity towards BBB has also been reported (Olivier et al., 1999). Moreover, drug-loaded nanoparticles released their content immediately and showed a pharmacological effect in no more than 60 min after their administration (Alyautdin et al., 1997).

To solve these problems, we entrapped PTX in MPEGylated poly(ε-caprolactone) (PCL) nanoparticles. PCL is a biodegradable polymer approved for human use by U.S. FDA and widely used in drug delivery applications (Pitt, 1990; Chawla and Amiji, 2002). Polymersomes made of MPEG–PCL conjugated with OX26 were recently shown to be able to cross the BBB after i.v. administrations (Pang et al., 2008).

Indeed, brain tumors have a compromised endothelial barrier which facilitates molecular transport (Grabb and Gilbert, 1995). Long-circulating nanoparticles were found either to accumulate at the margins of the brain tumor (Enochs et al., 1999) or to be taken up by the tumor cells and macrophages in tumor (Moore et al., 2000). In this study, we have compared the accumulation in brain tumor via the enhanced permeability and retention (EPR) effect of MPEGylated PCL nanoparticles (MPEG-NP) and non-MPEGylated PCL nanoparticles (NP) by in vivo real-time fluorescence imaging analysis. The anti-glioblastoma effect was also investigated using intracranial C6 glioblastoma mice model. In addition, we demonstrated that drug-loaded MPEGylated PCL long-circulating nanoparticles provided a sustained release of the embedded drug and higher or at least comparable in vitro cytotoxicity to that of Taxol injection against C6 glioblastoma cells.

2. Materials and methods

2.1. Materials, cell and animal

Methoxyl poly(ethylene glycol) (MPEG-OH, Mn is 2.0 kDa) and PCL (14.0 kDa) were purchased from Sigma (St. Louis, MO, USA). MPEG-PCL copolymer (12 kDa) with the content of 16.6% MPEG was synthesized by the ring opening polymerization as described before (Dong and Feng, 2004). Paclitaxel was purchased from Fujian south Bio-Engineering Co. Ltd. (Fujian, China). Taxol injection (Anzatax Injection Concentrate, 30 mg/5 ml) was produced by FH Faulding & Co. Ltd. trading as David Bull Lab (Melbourne, Australia). Cremophor EL was kindly supplied by BASF Ltd. (Shanghai, China). 3-(4,5-Dimethyl-thiazol-2-yl)-2,5-diphenyl-tetrazolium bromide (MTT) was purchased from Sigma (St. Louis, MO, USA). Penicillin–streptomycin, DMEM, fetal bovine serum (FBS) and 0.25% (w/v) trypsin–0.03% (w/v) EDTA solution were purchased from Gibco BRL (Gaithersberg, MD, USA). All the other solvents were analytical or chromatographic grade.

The C6 cell line was obtained from the Institute of Biochemistry and Cell Biology, Shanghai Institutes for Biological Sciences, Chinese Academy of Sciences (Shanghai, China). The cells were cultured in DMEM medium, supplemented with 10% FBS, 100 IU/ml penicillin and 100 μg/ml streptomycin sulfate. All the cells were cultured in incubators maintained at 37 °C with 5% CO_2 under fully humidified conditions. All experiments were performed on cells in the logarithmic phase of growth.

Male BALB/c nude mice (20 ± 2 g) and ICR mice (20 ± 2 g), supplied by Department of Experimental Animals, Fudan University (Shanghai, China), were acclimated at 25 °C and 55% of humidity under natural light/dark conditions for 1 week before experiment. All animal experiments were carried out in accordance with guidelines evaluated and approved by the ethics committee of Fudan University (Shanghai, China).

2.2. Preparation of drug-loaded nanoparticles

Nanoparticles were prepared using the O/W emulsion and evaporation technique (Mu and Feng, 2003; Peracchia et al., 1997). Briefly, 100 mg MPEG–PCL copolymer with PTX were dissolved in 3 ml dichloromethane (DCM). Next, 6 ml of 1% (w/v) sodium cholate solution was slowly poured into the solution and then sonicated at 200 W for 50 s (Xin zhi Biotechnology Co. Ltd., China). The resulted O/W emulsion was further diluted into 60 ml of a 0.5% aqueous sodium cholate solution and then stirred for 5 min at room temperature by a magnetic stirrer to solidify the nanoparticles. After that, the organic solvent was evaporated by rotary vacuum. The resultant bluish solution was filtrated through a 0.45 μm cellulose acetate filter membrane to remove the aggregates. The nanoparticles were concentrated by ultrafiltration (3000 MWCO Millipore, USA) and washed twice to remove excessive emulsifier. Finally, the suspension was kept at 4 °C for further use.

2.3. Characterization of PTX-loaded MPEG–PCL nanoparticles

2.3.1. Morphology

The morphology of the PTX-loaded nanoparticles was studied by transmission electron microscopy (Joel JEM-1230, Japan) after negative staining with phosphotungstic acid solution (2%, w/v).

2.3.2. Particle size and distribution

Mean particle size and size distribution were measured by the light scattering method using a Nicomp Zeta Potential/Particle Size (model 380XLS, NicompTM, Santa Barbara, CA, USA). The analyses were performed with 5 mW He–Ne laser (632.8 nm) at a scattering angle of 90° at 25 °C. Each sample was placed into a quartz cuvette and diluted to the appropriate concentration using deionized water to avoid multi-scattering phenomena. The reported experimental result of each sample was expressed as mean size ± SD for three separate experiments.

2.3.3. Drug-loading coefficient and encapsulation ratio

To investigate the drug loading coefficient (DL%) and encapsulation ratio (ER%), different amounts of PTX were co-dissolved with MPEG–PCL in the preparation process of nanoparticles. The drug-loaded nanoparticles were diluted by acetonitrile and the concentration of PTX was measured via HPLC on a system equipped with a LC-10ATVP pump, a SPD-10AVP UV detector (Shimadzu, Kyoto, Japan) and a HS2000 interface (Hangzhou Empire Science & Tech, Hangzhou, China). The mobile phase consisted of acetonitrile and ammonium acetate buffer solution (10 mM, pH 5.0) (50:45, v/v) was freshly prepared for each run and degassed before use. The reversed-phase column (Gemini 5 μm C18, 150 mm × 4.6 mm, Phenomenex, CA, USA) was used at room temperature. The flow rate was set at 1.0 ml/min and the detection wavelength was 230 nm. Sample solution was injected at a volume of 20 μl. The HPLC was calibrated with standard solutions of 0.5–50 μg/ml of PTX dissolved in acetonitrile (correlation coefficient of $R^2 = 0.9995$). The limit of quantification was 0.5 ng/ml. The coefficients of variation (CV) were

all within 3.5%. The drug loading coefficient (DL%) and encapsulation ratio (ER%) were obtained by the following equations (Zhang and Feng, 2006).

$$DL\% = \frac{\text{Weight of PTX in nanoparticles}}{\text{Weight of the feeding polymer and PTX}} \times 100\% \quad (1)$$

$$ER\% = \frac{\text{Weight of PTX in nanoparticles}}{\text{Weight of the feeding PTX}} \times 100\% \quad (2)$$

2.3.4. DSC

5 mg of PTX or freeze drying MPEG-NP/PTX sealed in standard aluminum pans with lids was studied by DSC (DSC 204//1/Gphoenix®, German) under liquid nitrogen at a flow rate of 20 ml/min. The temperature ramp speed was set at 10 °C/min from 20 to 270 °C. Indium was used as the standard reference material to calibrate the temperature and energy scales of the DSC instrument (Hu et al., 2007).

2.3.5. Stability studies

In order to evaluate the stability of the nanoparticles, PTX-loaded nanoparticles suspension was diluted by PBS (pH 7.4) or DMEM medium containing 10% FBS and then kept at 4 °C. The particle size was determined by DLS every 3 days.

2.4. In vitro PTX release

In order to create pseudo-sink conditions, the in vitro release behavior of PTX from MPEG–PCL nanoparticles were monitored in an aqueous medium containing 1 M sodium salicylate by dialysis method (Han et al., 2006; Zhang et al., 2009). 1 ml of PTX-loaded nanoparticle solution (containing 0.1 mg PTX) was introduced into a dialysis bag (MWCO = 14,000 Da, Greenbird Inc., Shanghai, China) and the end sealed dialysis bag was submerged fully into 50 ml of 1 M sodium salicylate solution at 37 °C with stirring at 100 rpm for 96 h. At appropriate time intervals (1, 2, 4, 6, 8, 10, 12, 24, 48, 72, 96 h), 0.2 ml aliquots were withdrawn and replaced with an equal volume of fresh medium. The concentration of PTX in samples was determined by HPLC as described above with correction for the volume replacement.

To investigate the MPEGylation effect on the release profiles, PTX-loaded non-MPEGylated PCL nanoparticles (NP/PTX) were also studied. Meanwhile, PTX release from stock solution (in DMSO) was also conducted under the same condition as controls.

2.5. In vitro anti-tumor efficacy of nanoparticles

C6 Cells were seeded at the density of 5.0×10^3 cells per well in 96-well plate. After 24 h incubation, the growth medium was replaced with 200 μl medium containing respective, MPEG-NP/PTX, NP/PTX and Taxol injection with various concentrations. After 24, 48 and 72 h incubation, cell survival was then measured using tetrazolium salt MTT assay. 180 μl of fresh growth medium and 20 μl of MTT (5 mg/ml) solution were added to each well. The plate was incubated for an additional 4 h, and then 200 μl of DMSO was added to each well to dissolve any purple formazan crystals formed. The plates were vigorously shaken before measuring the relative color intensity. The absorbance at 570 nm of each well was measured by a microplate reader (Thermo Multiskan MK3, USA).

In order to evaluate the toxicity of the excipients, cytotoxicity of the blank nanoparticles and Cremophor EL with concentration ranging from 0.1 to 2000 μg/ml was also conducted under the same method as above.

2.6. In vivo real-time imaging analysis

In vivo real-time fluorescence imaging analysis was used to evaluate the effect of MPEGylation on the biodistribution of nanoparticles. C6 cells (1.0×10^5 cells suspended in 5 μl PBS) were implanted into the right striatum (1.8 mm lateral to the bregma and 3 mm of depth) of male BALB/c nude mice by using a stereotactic fixation device with mouse adaptor. MPEG-NP and NP were labeled by Dir (Invitrogen, USA). In brief, Dir was co-dissolved with MPEG–PCL or PCL in DCM during nanoparticles preparation. Then, the free Dir was removed via CL-4B column (Hanhong Chemical Co. Ltd., China). The intracranial C6 tumor bearing mice were injected with 100 μl of Dir encapsulated (0.5%) MPEG-NP or NP via tail vein 16 days after implantation. The mice were anesthetized with i.p. administered 10% chloral hydrate and placed on an animal plate heated to 37 °C. The fluorescent scans (from 620 nm to 900 nm) were performed at 1, 2, 6, 12, 24 and 48 h post i.v. using an in vivo image system (CRI, MA, USA). A quantification of fluorescence intensity was recorded as total photons per centimeter squared per steradian (p/s/cm^2/sr) per tumor-bearing brain.

2.7. In vivo anti-tumor efficacy

The survival times of brain tumor-bearing mice were investigated using male ICR mice of 20 ± 2 g body weight. C6 cells (1.0×10^5 cells suspended in 5 μl PBS) were implanted into the right striatum (1.8 mm lateral to the bregma and 3 mm of depth) of mice by using a stereotactic fixation device with mouse adaptor. The mice were randomly divided into four groups and treated with 100 μl of MPEG-NP/PTX, NP/PTX, Taxol at doses of 10 mg/kg on a PTX basis and physiological saline days 7, 9, 11, 13 after implantation. The body weight was monitored every other day and the death was recorded as occurring on the following day.

3. Result and discussion

3.1. Morphology, particles size and zeta potential

Since particle size is an important property of particles that not only does it affect endocytosis by tumor cells but also influences its accumulation in tumor tissue via EPR effect, the nanoparticles should be small enough to evade detection and destruction by the reticulo-endothelial system (RES). In this study, the average size of nanoparticles is illustrated in Fig. 1a and b. The particle size of MPEG-NP is smaller significantly than that of NP. Though the particle size of both carries is different, they are around or less than 100 nm with narrow distribution (PDI between 0.11 and 0.16). Such ranged nanoparticles may accumulate more readily in tumor due to the EPR effect (Zhu et al., 2010). However, the bigger nanoparticles may be recognized by RES more easily. Loading nanoparticle with PTX did not visibly affect particle size and size distribution. As seen from Fig. 1c, the nanoparticles exhibited spherical shape of moderate uniform particle size and the particle size measured from the TEM images was in good agreement with that measured by the laser scattering technique.

From Table 1, we can see that the zeta potential of MPEG-NP is close to neutral (about −3.75 ± 0.52 mV). In contrast, the zeta potential for NP is −15.28 ± 2.31 mV. In general, the negatively

Table 1
Particles size and zeta potential of the nanoparticles ($n = 3$).

Nanoparticles	Size (nm)	Polydispersity	Zeta potential (mV)
MPEG-NP	69.3 ± 1.2	0.12 ± 0.05	−3.75 ± 0.52
NP	104 ± 3.6	0.11 ± 0.06	−15.28 ± 2.31
MPEG-NP/PTX	72.5 ± 2.2	0.14 ± 0.02	−3.08 ± 0.94
NP/PTX	108 ± 1.6	0.16 ± 0.05	−13.59 ± 1.58

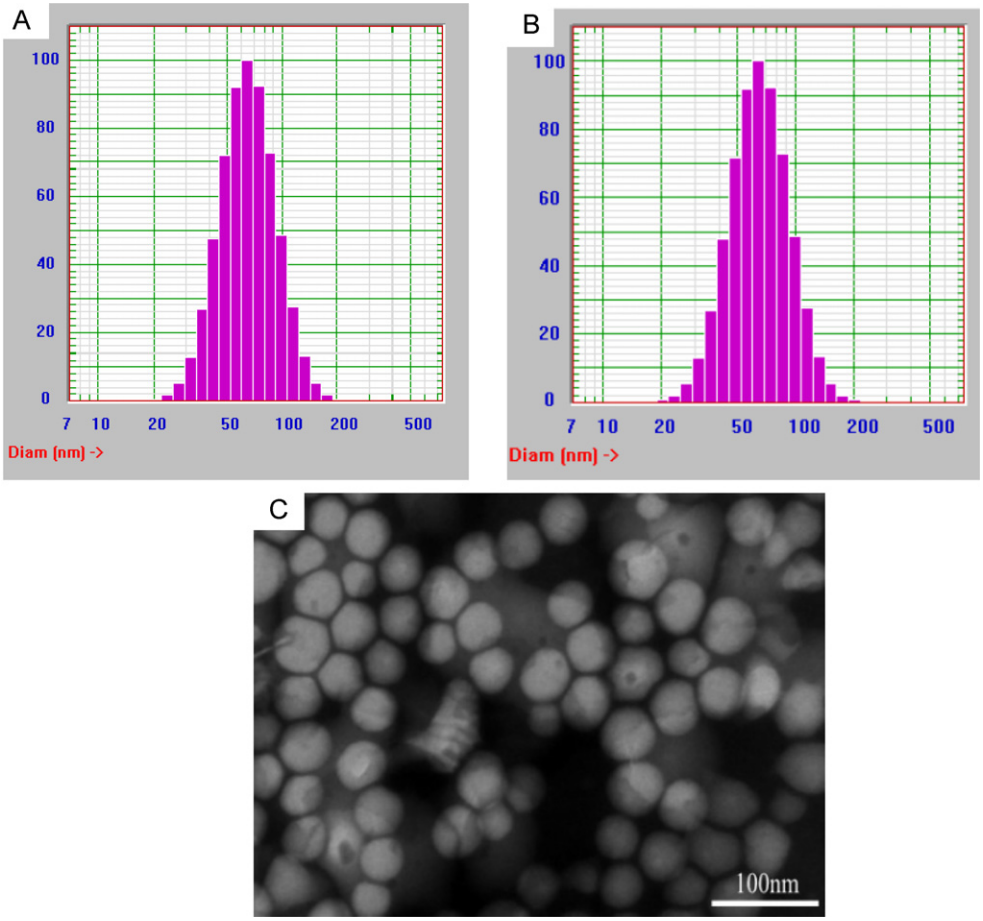

Fig. 1. (A) Nanoparticles size and size distribution of empty MPEG–PCL nanoparticles and (B) PTX-loaded MPEG–PCL nanoparticles, (C) TEM image of PTX-loaded MPEG–PCL nanoparticles, the bar is 100 nm.

charged cell membrane has a tendency to absorb positive charged or neutral nanoparticles (Hu et al., 2007). So the electronic repulsion between NP and tumor cells may result in fewer nanoparticles being uptaken to tumor cells compared to MPEG-NP. The zeta potential of the PTX-loaded nanoparticles was slightly lower than that of blank nanoparticles probably due to the partial absorption of PTX on the surface of nanoparticles during preparation process. However, this trend was not statistically significant ($p = 0.16$).

3.2. Drug-loading coefficient and encapsulation ratio

The drug-loading coefficient and encapsulation efficiency of MPEG-NP at different PTX feeding were shown in Fig. 2. With increasing of PTX feeding, the encapsulation efficiency decreased, but the drug-loading coefficient increased firstly and then decreased sharply, which was consistent with the previous studies (Wang et al., 2007; Li et al., 2009). It suggested that the hydrophobic interaction between PTX molecules exceeded that between drug and copolymers as the amount of PTX increased (Zhang et al., 2009). Therefore, maximum encapsulation efficiency was in group with minimum drug-loading coefficient. Fortunately, the drug-loading coefficient could reach $8.2 \pm 0.6\%$ along with $90.4 \pm 2.3\%$ encapsulation efficiency when adding 10 mg PTX. In the following study, the feeding ratio of PTX was fixed at 10 mg when 100 mg copolymer was used.

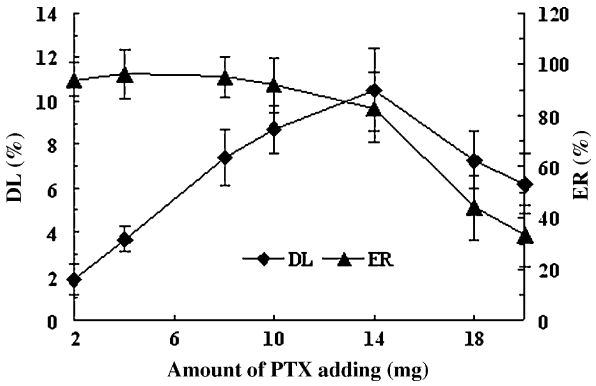

Fig. 2. Drug-loading content (DL%) and encapsulation ratio (ER%) of nanoparticles as a function of amount of PTX adding ($n = 3$).

3.3. DSC

The status of incorporated drug in nanoparticles is very important of a drug delivery system (Soo et al., 2002). Therefore, we investigated the physical status of the drug encapsulated in polymeric matrix by DSC. As shown in Fig. 3, PTX exhibited a melting peak at around 244.6 °C, which implies that PTX is in crystal status. After encapsulation inside the nanoparticles, the melting peak of PTX disappeared. It could be concluded that majority of PTX formulated in MPEG–PCL nanoparticles were in an amorphous or disorder crystalline phase of a molecular dispersion or a solid solution state in the polymer matrix (Hu et al., 2007).

3.4. In vitro stability of PTX-loaded nanoparticles

To investigate the stability of nanoparticles, the PTX-loaded nanoparticles suspension was diluted by PBS (pH 7.4) or DMEM

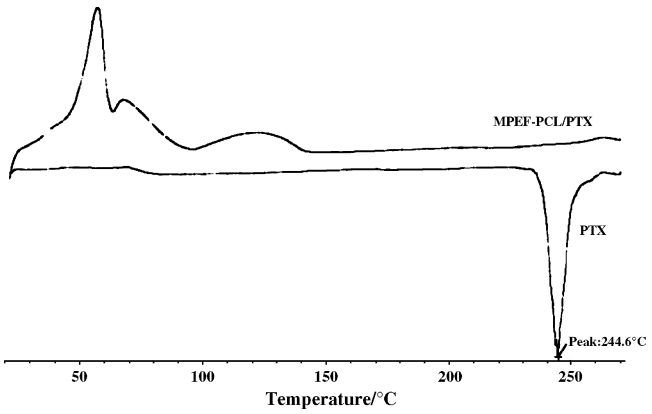

Fig. 3. Differential scanning calorimetry (DSC) thermograms of PTX and PTX-loaded MPEG-PCL nanoparticles.

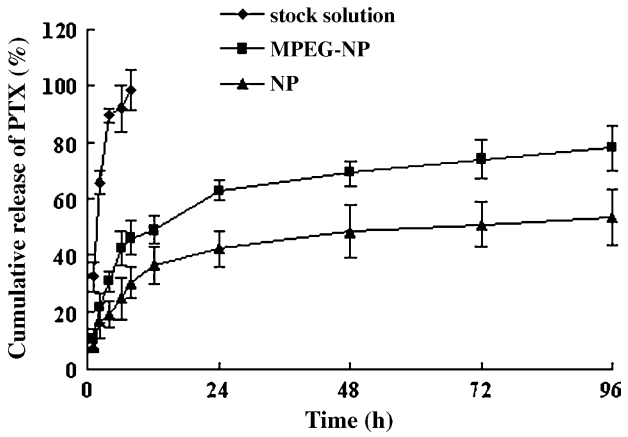

Fig. 5. Release profiles of PTX from MPEG-NP/PTX and NP/PTX in 1 M sodium salicylate medium at 37 °C. Each point represents average ± SD ($n = 3$).

medium containing 10% FBS and then kept at 4 °C. There were no notable aggregates in the PTX-loaded MPEG–PCL nanoparticles solution of PBS or DMEM medium containing 10% FBS and the mean diameter of nanoparticles did not remarkably changed during the period of 21 days (Fig. 4), indicating the thermodynamic stability of PTX encapsulated nanoparticles in aqueous condition. The probable reason was that the hydrophilic PEG shell could prevent aggregation among particles and binding between particles and plasma protein, which implies that MPEGylated PCL nanoparticles may avoid opsonisation to overcome recognization and removal by the MPS.

3.5. In vitro PTX release from nanoparticles

The in vitro cumulative release profiles of PTX from different formulations are shown in Fig. 5. The maximum concentration of PTX in the medium was 2.0 μg/ml, while the solubility of PTX in 1 M sodium salicylate medium was 28.1 μg/ml (Cho et al., 2004), and thus good sink conditions were respected. In addition, prior to conducting these release assays, PTX release from stock solution was investigated as positive controls. It was found nearly 90% of PTX in stock solution was released within the first 4 h. This suggested that PTX could freely diffuse through the dialysis membrane. From Fig. 5, we can see that MPEG-NP/PTX and NP/PTX present biphases release behavior. After the initial burst release for about 12 h, the release rate of PTX slowed down and became an almost zero-order release. PTX released in the first 12 h was equivalent to 49.2 ± 4.8% for MPEG-NP and 36.5 ± 6.9% for NP of the initial drug loading of nanoparticles. After 96 h, the PTX release was 77.9 ± 7.2% for MPEG-NP and 53.5 ± 8.9% for NP. The burst release of PTX might be due to the diffusion of PTX that was adsorbed on the surface of nanoparticles. Similar burst effect was also observed in other studies (Jugminder and Mansoor, 2002; Mu and Feng, 2003; Hu et al., 2007; Danhier et al., 2009).

Compared to NP/PTX, the drug release rate and cumulative release amount of MPEG-NP/PTX exceeded that of NP/PTX. The phenomenon may be explained as follows: first, the smaller particle size of MPEG-NP resulting in greater surface area than NP, which accelerates PTX diffusion and dissolution from polymer matrix. Second, the PTX binding affinity with PCL segment is stronger than MPEG–PCL segment. Third, NP/PTX may be prone to aggregate in electrolyte solution, which hampers PTX release from nanoparticles, while the neutral PEG shell of MPEG-NP creates a barrier layer to block the aggregation among particles in sodium salicylate solution. In addition, maybe there are other factors affecting the PTX release behavior of nanoparticles include polymer molecular weight, degradation rate, crystallinity, etc. (Ratner et al., 1996; Kim et al., 2000).

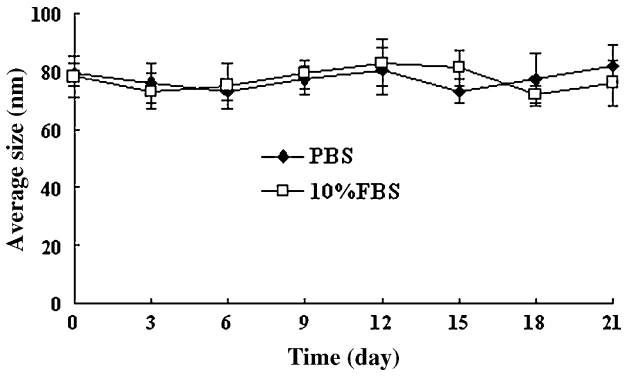

Fig. 4. Particle size of PTX-loaded MPEG–PCL nanoparticles at 4 °C in PBS and DMEM medium containing 10% FBS as a function of time. Data represents mean ± SD ($n = 5$).

3.6. In vitro cytotoxicity assay

In vitro biocompatibility study of Cremophor EL and empty nanoparticles were carried out using C6 cell line. In the concentration ranges (0.1–100 μg/ml) used in this study, the cytotoxic effects of blank NP and MPEG-NP were negligible, as shown in Fig. 6A, C and E. It was also reported MPEG–PCL nanoparticles had no cytotoxicity on HepG2 cell within 5 mg/ml after incubation for 24 h (Hu et al., 2007). However, it was shown that blank nanoparticles displayed increasing cytotoxicity as the concentration and incubation time increased in this study. The growth inhibition of both NP and MPEG-NP against C6 (44.53 ± 3.9%, 48 ± 5.60% respectively) was significant at 2 mg/ml after incubation for 72 h, but Cremophor EL exhibited much higher cytotoxicity than that of blank nanoparticles at identical concentration. The viable of C6 cells after 72 h exposure with Cremophor EL was 15.24 ± 7.19%. As reported previously, Cremophor EL was significantly cytotoxic at concentration above 1 mg/ml (Liebmann et al., 1993, 1994; Zhang et al., 2010).

In addition, in vitro cytotoxicity of PTX-loaded nanoparticles were investigated and compared with that of Taxol injection using C6 cells (Fig. 6B, D and F). The IC_{50} values at 24 h of Taxol, NP/PTX and MPEG-NP/PTX were 11.9 ± 1.63, 17.7 ± 1.72, 15.7 ± 1.46 μg/ml, respectively. After 72 h treatment, the IC_{50} values of Taxol, NP/PTX and MPEG-NP/PTX were decreased to 1.94 ± 0.35, 1.6 ± 0.21 and 1.4 ± 0.15 μg/ml, respectively. It was straightforward to understand that both incubation time and concentration played a major

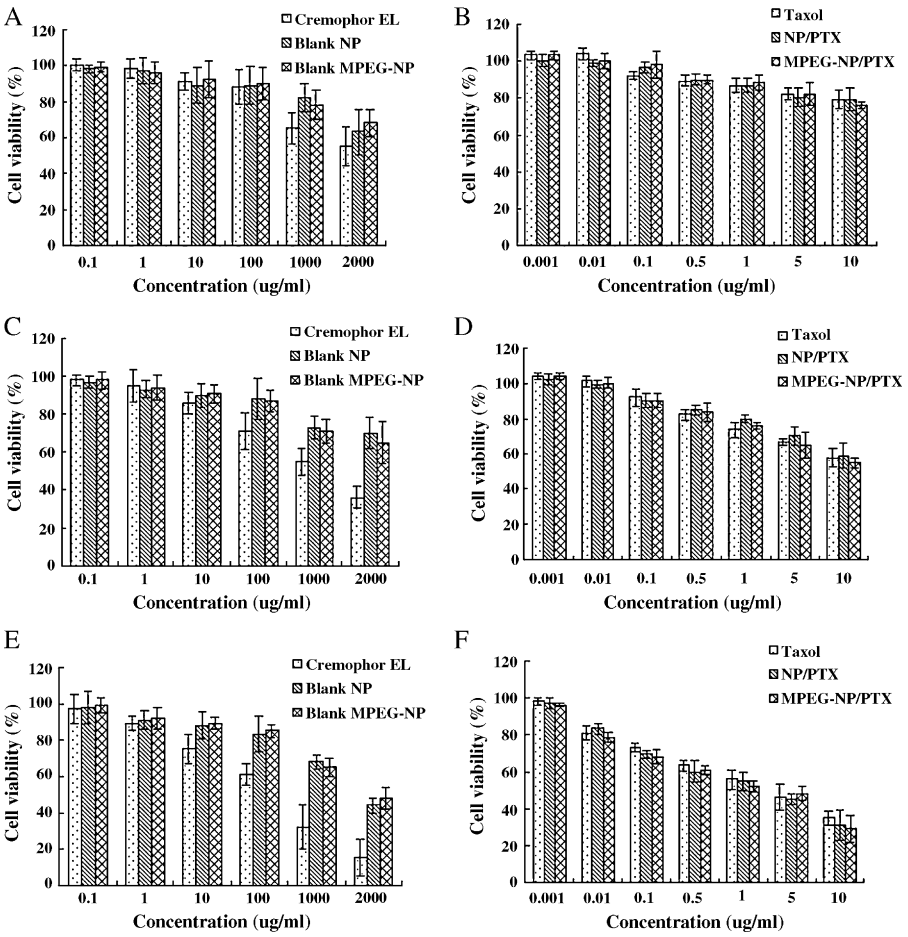

Fig. 6. Viability of C6 cells as a function of varying concentrations of excipients (Cremophor EL and blank nanoparticles) at (A) 24 h, (C) 48 h and (E) 72 h; in vitro cytotoxicy of Taxol and PTX-loading nanoparticles at various concentrations of PTX against C6 cells at (B) 24 h, (D) 48 h and (F) 72 h. Each point represents mean ± SD ($n = 3$).

role in the in vitro cytotoxicity of PTX, viz. higher drug concentration and longer incubation time would cause lower cell viability. For longer incubation periods, a larger number of cells could enter the G2/M phase during which PTX was more active (Schiff et al., 1979).

It is obvious that the cell viability was less inhibited by PTX-loaded nanoparticles than by Taxol at 24 h incubation ($p < 0.05$). The reason is that Taxol is immediately available for the cells by the passive diffusion while drug-loading nanoparticles internalized into cells via endocytosis or phagocytosis (Ambruosi et al., 2005; Steiniger et al., 2004) although some PTX in the core are released from nanoparticles in the extracellular space (Chen et al., 2008). Fortunately, it can observed that the higher or comparable effectiveness of nanoparticle versus Taxols at 72 h incubation. Furthermore, if we take into account that for the nanoparticles formulation, it is a fraction, instead of the whole loaded drug, that is released out and acts on the cells at specific intervals, the PTX-loaded nanoparticles should be considered more effective (Dong and Feng, 2007). As shown in Fig. 5, 75 ± 2.4% and 51 ± 3.1% of the drug loaded in the MPEG-NP and NP were released after 72 h respectively. However, this kind of modification is unrealistic. Moreover, in vivo and in vitro results might be very much different. It should be emphasized that in the case of Taxol a significant cytotoxicity effect was attributed to the excipient Cremophor EL, whereas in the case of PTX-loaded nanoparticles the cytotoxicity observed was only attributed to PTX. It is consistent with other reports data that the incorporation of PTX into nanoparticles could enhance its anticancer activity compared to Taxol (Breuning et al., 2008).

3.7. In vivo real-time imaging analysis

In order to observe in vivo biodistribution of MPEGylated poly(ε-caprolactone) nanoparticles, DiR-labeled MPEG-NP were given intravenously into C6 glioblastoma bearing mice through the tail vein and time-dependant biodistribution was observed using non-invasive NIRF imaging in live animals. As shown in Fig. 7A, the fluorescence signal was viewed in the tumor-bearing brain as early as 1 h after injection and exhibited a maximum fluorescence signal at 12 h post-injection with decrease after 24 h post-injection. Compared with NP group, the fluorescence signal of MPEG-NP group was much stronger at any time post-injection. From Fig. 7B we can see the AUC of MPEG-NP group was 4 times that of the NP group.

The in vitro release kinetics of DiR-loaded PCL nanoparticles and MPEG–PCL nanoparticles was investigated by dialysis method. It indicated that only less than 1% of DiR released from the nanoparticles within 48 h (data not shown). Therefore, the DiR combining with nanoparticles together penetrated into brain but not free DiR in the in vivo real-time imaging analysis. Micelles labeled by DiR used the same method were reported in other references (Zhan et al., 2010; Shen et al., 2010). The mechanism by which nanoparticles penetrated across BBB has so-far not been totally explained and has attracted numbers of debates. In this study, it would be that polipoproteins E and AI (Apo E and AI) played an important role in the nanoparticles cross BBB transport (Zensi et al., 2009). After injection into the blood stream Apo E and AI were absorbed onto the surface of MPEG–PCL nanoparticles. The apolipoprotein-modified "Trojan Horses" could interact with these apolipoprotein receptors at the BBB and result in transcytosis into the brain (Kreuter

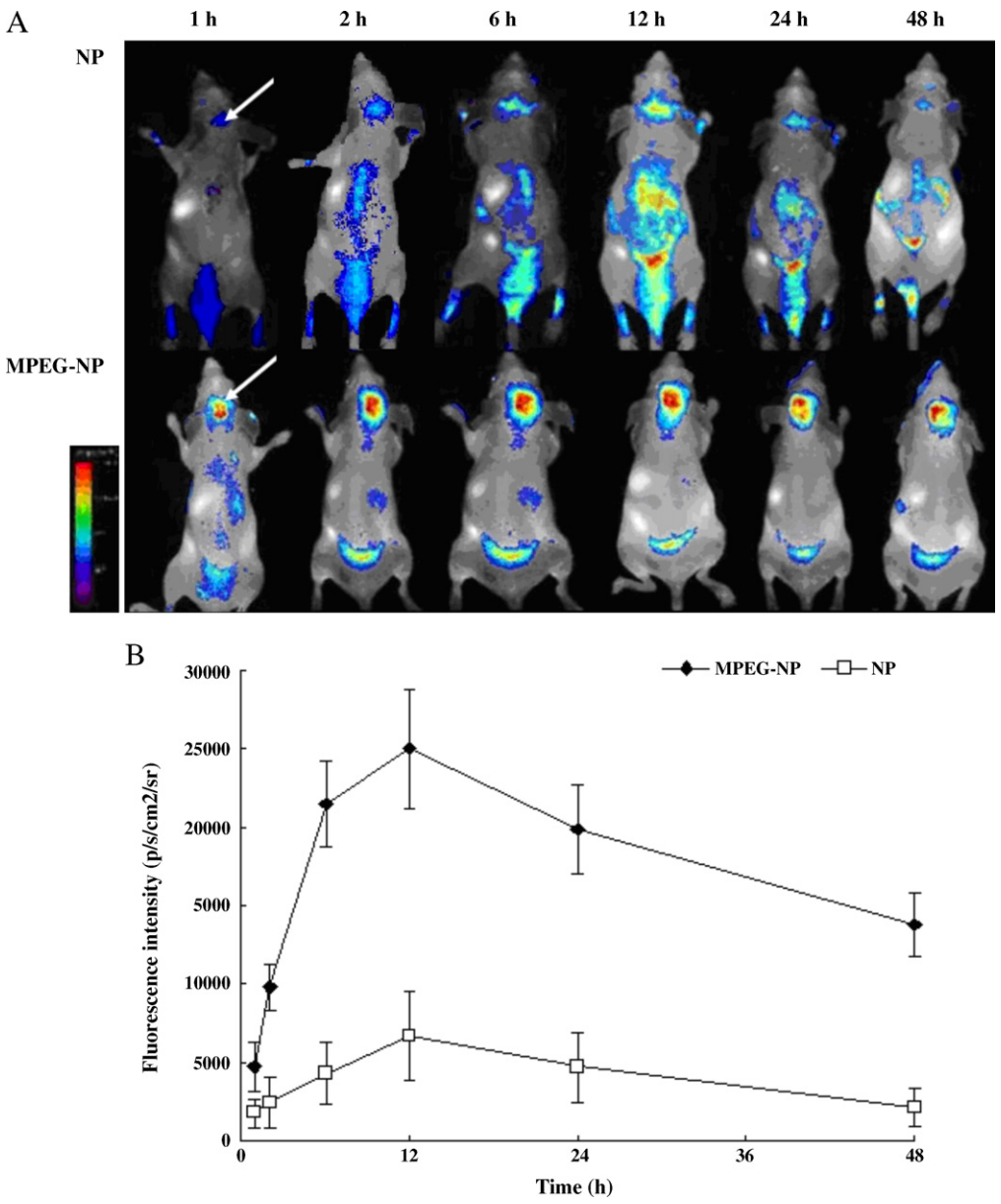

Fig. 7. (A) In vivo fluorescence imaging of intracranial C6 glioma tumor-bearing nude mice after intravenous injection of DIR labeled nanoparticles. (B) The total photon counts per centimeter squared per steradian (p/s/cm^2/sr) per each tumor-bearing brain as a function of time ($n = 3$).

et al., 2002) and then accumulated in brain tumor tissue via EPR effect. The proposal was testified by the observation of nanoparticles adsorbed or covalently bound Apo E or AI across BBB (Kreuter et al., 2007; Petri et al., 2007). Another reason might be that grafted PEG chains create a barrier layer to block the adhesion of opsonins present in the blood serum so that the particles can remain camouflaged or invisible to phagocytic cells and exhibit more accumulation in tumor (Owens and Peppas, 2006). On the contrary, PCL nanoparticles could not absorb Apo E and AI but complement components, immunoglobulins and immunoglobulin-like proteins, which resulted in activation of the complement system and recognization by RES (Gaucher et al., 2009). Therefore, the fate of nanoparticles in vivo is related with protein adsorption more than the bare material properties of the particle itself (Walczyk et al., 2010).

It is reported the BBB penetration effect of PEG–PCL polymersomes conjugated with mouse-anti-rat monoclonal antibody OX26 (OX26-PO) increased by 2.6-fold compared with that of PEG–PCL polymersomes (PO) in normal Sprague–Dawley rat model (Pang et al., 2008). OX26 is a kind of transferrin receptor monoclonal antibody. So OX26-PO penetrated across BBB through the endogenous transferrin receptor-mediated transcytosis. However, in this study, glioblastoma-bearing mice model was used to evaluate the target effect of MPEG–PCL nanoparticles. It is known that BBB is impaired to some extent of xenograft glioblastoma model (De Vries et al., 2009). Therefore, MPEG–PCL nanoparticles could target to brain tumor tissue via the EPR effect where nanoparticles spontaneously accumulate in the pathological area due to the hydrophilic surface and long blood duration. Based on normal Sprague Dawley rat model, the BBB penetration effect of OX26-PEG–PCL polymersomes must exceed that of PEG–PCL nanoparticles.

3.8. In vivo anti-tumor efficacy

The anti-glioblastoma effect of MPEG-NP/PTX in close comparison with those of saline, NP/PTX and Taxol was demonstrated by the survival time of intracranial C6 glioblastoma-bearing mice in Fig. 8A. We can see that the antitumor efficacy of MPEG-NP/PTX was

Table 2
In vivo effects of PTX formulations on intracranial C6 glioblastoma mice model ($n = 5$).

Groups	Dose (mg/kg)	MST (days)	Median (days)	Compare with saline [a]	Compare with Taxol [a]	Compare with NP/PTX [a]
Saline	–	18 ± 2.2	17	–	–	–
Taxol	10	20 ± 1.5	20	$p > 0.05$	–	–
NP/PTX	10	23 ± 1.6	23	**	$p > 0.05$	–
MPEG-NP/PTX	10	28 ± 4.0	26	**	**	**

MST: mean survive time.
[a] ** $p < 0.01$ of log-rank analysis.

superior to those of other treatments. As shown in Table 2, the mean survival time of MPEG-NP/PTX group, NP/PTX group, Taxol group and physiological saline group were 18, 20, 23 and 28 days, respectively. Compared to physiological saline, Taxol group displayed no significant prolongation in the survival time ($p > 0.05$) through log-rank analysis. When compared to Taxol, MPEG-NP/PTX group ($p < 0.01$) significantly prolonged the survival time. But NP/PTX group resulted in no significant prolongation in the survival time compared to Taxol ($p > 0.05$). In a word, the antitumor efficacy of MPEGylated nanoparticles formulation was superior to those of Taxol injection and non-MPEGylated nanoparticles for intracranial C6 glioblastoma model. These results might be explained by the increased local concentration of PTX in the tumor tissue, since accumulation of MPEG-NP/PTX in tumors was favored by their long circulation time and EPR effect. Thus, MPEG-NP/PTX appeared to retain the desirable effects of passive targeting because of the long PEG shell. Another reason could be that BBB was destructed to some extent by tumor growth (Stewart et al., 1987).

In order to evaluate the safety of these PTX formulations, body weight was monitored as a marker of overall toxicity. The change in body weight was recorded in 16 days because the first mouse in saline group died on day 17 after implantation. From Fig. 8B, we can see that there was no serious body weight loss in mice after PTX-loaded nanoparticles and Taxol treatment. Although there were some slight weight loss in Taxol group and NP/PTX group 10 days after tumor implantation, it was not induced by PTX formulation but tumor growth because the same case was observed in the saline treatment. On the contrary, the MPEG-NP/PTX group mice gained weight during the observed period. These results implied that MPEGylated PCL nanoparticle was a safe and effective drug deliver system for advanced glioblastoma treatment.

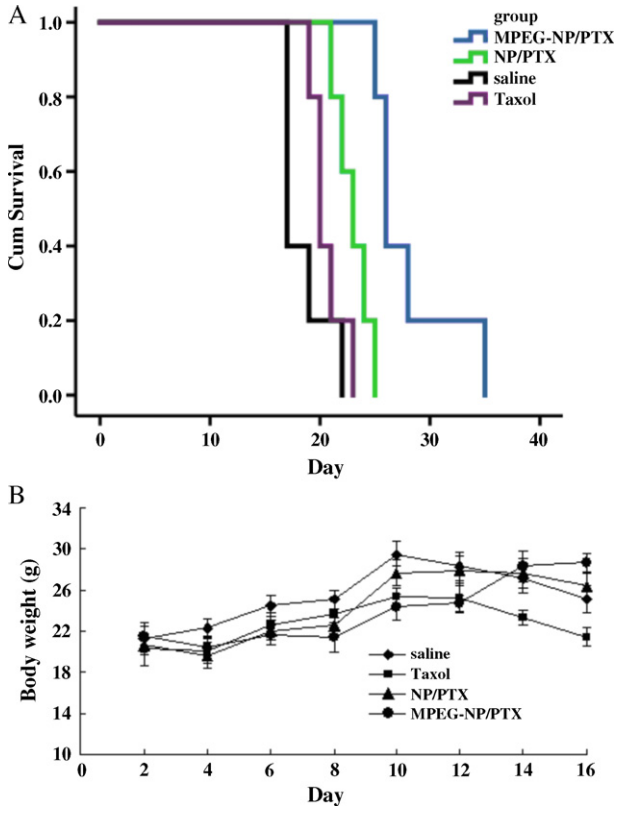

Fig. 8. (A) Kaplan–Meier survival curve of mice bearing intracranial C6 glioblastoma, (B) change in body weight of animals as a function of time in bearing intracranial C6 glioblastoma mice ($n = 5$).

The anticancer effect and the survive time may relate with the dosage regime of PTX formulations. Therefore, the dosage regime of PTX formulations was determined through preliminary test, in which the intracranial C6 glioblastoma-bearing ICR mice (18–22 g) were given PTX formulations through tail vein of 5, 10, 15, 20 mg/kg to determine the tolerance dose. It was found that mice were prone to die of 15 and 20 mg/kg for Taxol. But it was relatively safe for 5, 10 mg/kg. So, 10 mg/kg was adopted as the dosage of PTX formulation. Zhang et al. (2010) also gave the same dosage of PTX. According to our experiences and preliminary tests, the advanced stage of intracranial C6 glioblastoma forms on days 6–7 after implanting and the mice will start to die on days 15 after implanting without any anti-canner treatment. It is indicating that the treatment time span is no more than 10 days. To give four times PTX formulations and start to give on day 7 after implanting, it is the only choice to give PTX formulation in every two days.

4. Conclusion

In this study, MPEGylated PCL nanoparticles containing PTX were prepared by the emulsion and evaporation technique. The optimized formulation showed the particle size around 70 nm with ideal drug loading coefficient and encapsulation ratio. The MPEG–PCL nanoparticles possess excellent stability during 21-day storage at 4 °C. C6 glioblastoma cell viability studies showed that MPEG-NP/PTX could produce higher or at least comparable cytotoxicity than Taxol injection. As demonstrated by in vivo real-time fluorescence imaging analysis in intracranial C6 glioblastoma bearing mice, the MPEGylated PCL nanoparticles displayed much stronger fluorescence signal in tumor tissue and larger AUC than non-MPEGylated PCL nanoparticles. The therapeutic improvement of MPEG-NP/PTX in vivo against intracranial C6 glioblastoma was also obtained based on the effect of passive tumor targeting. Our proof-of-concept in vitro and in vivo valuation shows that the MPEG–PCL nanoparticles seem be a potential drug delivery system of PTX for advanced glioblastoma treatment.

Acknowledgements

We are grateful for the financial supports from the National Basic Research Program of China 973 program (2007CB935802); National Natural Science Foundation of China (30873177) and National Science and Technology Major Project (2009ZX09310-006).

References

Allard, E., Passirani, C., Benoit, J.P., 2009. Convection-enhanced delivery of nanoparticles for the treatment for brain tumors. Biomaterials 30, 2302–2318.

Alyautdin, R.N., Petrov, V.E., Langer, K., Berthold, A., Kharkevich, D.A., Kreuter, J., 1997. Delivery of loperamide across the blood–brain barrier with polysorbate 80-coated polybutylcyanoacrylate nanoparticles. Pharm. Res. 14, 325–328.

Ambruosi, A., Khalansky, A.S., Yamamoto, H., Gelperina, S.E., Begley, D.J., Kreuter, J., 2006. Biodistribution of polysorbate 80-coated doxorubicin-loaded [^{14}C]-poly(butyl cyanoacrylate) nanoparticles after intravenous administration to glioblastoma-bearing rats. J. Drug Target. 14, 97–105.

Ambruosi, A., Yamamoto, H., Kreuter, J., 2005. Body distribution of polysorbate-80 and doxorubicin-loaded [^{14}C]-poly(butyl cyanoacrylate) nanoparticles after i.v. administration in rats. J. Drug Target. 13, 535–542.

Breuning, M., Bauer, S., Goepferich, A., 2008. Polymers and nanoparticles: intelligent tools for intracellular targeting? Eur. J. Pharm. Biopharm. 68, 112–128.

Calvo, P., Gouritin, B., Chacun, H., Desmaële, D., D'Angelo, J., Noel, J., Georgin, D., Fattal, E., Andreux, J.P., Couvreur, P., 2001. Long-circulating PEGylated polycyanoacrylate nanoparticles as new drug carrier for brain delivery. Pharm. Res. 18, 1157–1166.

Calvo, P., Gouritin, B., Villarroya, H., Eclancher, F., Giannavola, C., Klein, C., Andreux, J.P., Couvreur, P., 2002. Quantification and localization of PEGylated polycyanoacrylate nanoparticles in brain and spinal cord during experimental allergic encephalomyelitis in the rat. Eur. J. Neurosci. 15, 1317–1326.

Chang, S.M., Kuhn, J.G., Robins, H.I., Schold, S.C., Spence, A.M., Berger, M.S., Mehta, M., Pollack, I.F., Rankin, C., Prados, M.D., 2001. A phase II study of paclitaxel in patients with recurrent malignant glioma using different doses depending upon the concomitant use of anticonvulsants: a North American brain tumor consortium report. Cancer 91, 417–422.

Chawla, J.S., Amiji, M.M., 2002. Biodegradable poly(ε-caprolactone) nanoparticles for tumortargeted delivery of tamoxifen. Int. J. Pharm. 249, 127–138.

Chen, H.T., Kim, S., Li, L., Wang, S.Y., Park, K., Cheng, J.X., 2008. Release of hydrophobic molecules from polymer micelles into cell membranes revealed by Förster resonance energy transfer imaging. Proc. Natl. Acad. Sci. U.S.A. 105, 6596–6601.

Cho, Y.W., Lee, J., Lee, S.C., 2004. Hydrotropic agents for study of in vitro paclitaxel release from polymeric micelles. J. Control. Release 97, 249–257.

Danhier, F., Lecouturier, N., Vroman, B., Jérôme, C., Marchand-Brynaert, J., Feron, O., Préat, V., 2009. Paclitaxel-loaded PEGylated PLGA-based nanoparticles: in vitro and in vivo evaluation. J. Control. Release 133, 11–17.

Desai, A., Vyas, T., Amiji, M., 2008. Cytotoxicity and apoptosis enhancement in brain tumor cells upon coadministration of paclitaxel and ceramide in nanoemulsion formulations. J. Pharm. Sci. 97, 2745–2756.

De Vries, N.A., Beijnen, J.H., Tellinge, O.V., 2009. High-grade glioma mouse models and their applicability for preclinical testing. Cancer Treat. Rev. 35, 714–723.

Dong, Y.C., Feng, S.S., 2004. Methoxy poly(ethylene glycol)–poly(lactide) (MPEG–PLA) nanoparticles for controlled delivery of anticancer drugs. Biomaterials 25, 2843–2849.

Dong, Y.C., Feng, S.S., 2007. In vitro and in vivo evaluation of methoxy polyethylene glycol–polylactide (MPEG–PLA) nanoparticles for small-molecule drug chemotherapy. Biomaterials 28, 4154–4160.

Enochs, W.S., Harsh, G., Hochberg, F., Weissleder, R., 1999. Improved delineation of human brain tumors on MR images using a long-circulating, superparamagnetic iron oxide agent. J. Magn. Reson. Imaging 9, 228–232.

Friese, A., Seiller, E., Quack, G., Lorenz, B., Kreuter, J., 2000. Increase of the duration of the anticonvulsive activity of a novel NMDA receptor antagonist using poly(butylcyanoacrylate) nanoparticles as a parenteral controlled release system. Eur. J. Pharm. Biopharm. 49, 103–109.

Gaucher, G., Asahina, K., Wang, X.D., Leroux, J.C., 2009. Effect of poly(*N*-vinylpyrrolidone)-block-poly(D,L-lactide) as coating agent on the opsonization, phagocytosis, and pharmacokinetics of biodegradable nanoparticles. Biomacromolecules 10, 408–416.

Grabb, P.A., Gilbert, M.R., 1995. Neoplastic and pharmacological influence on the permeability of an in vitro blood–brain barrier. J. Neurosurg. 82, 1053–1058.

Gulyaev, A.E., Gelperina, S.E., Skidan, I.N., Antropov, A.S., Kivman, G.Y., Kreuter, J., 1999. Significant transport of doxorubicin into the brain with polysorbate 80-coated nanoparticles. Pharm. Res. 16, 1564–1569.

Han, L.M., Guo, J., Zhang, L.J., Wang, Q.S., Fang, X.L., 2006. Pharmacokinetics and biodistribution of polymeric micelles of paclitaxel. Acta Pharmacol. Sin. 27, 747–753.

Heimans, J.J., Vermorken, J.B., Wolbers, J.G., Eeltink, C.M., Meijer, O.W.M., Taphoorn, M.J.B., 1994. Paclitaxel concentrations in brain tumor tissue. Ann. Oncol. 5, 951–953.

Hu, Y., Xie, J.W., Tong, Y.W., Wang, C.H., 2007. Effect of PEG conformation and particle size on the cellular uptake efficiency of nanoparticles with the HepG2 cells. J. Control. Release 118, 7–17.

Jugminder, S.C., Mansoor, M.A., 2002. Biodegradable poly(ε-caprolactone) nanoparticles for tumortargeted delivery of tamoxifen. Int. J. Pharm. 249, 127–138.

Kim, S.Y., Ha, J.C., Lee, Y.M., 2000. Poly(ethylene oxide)–poly(propylene oxide)–poly(ethylene oxide)/poly(e-caprolactone) (PCL) amphiphilic block copolymeric nanospheres. II. Thermo-responsive drug release behaviors. J. Control. Release 65, 345–358.

Kreuter, J., Hekmatara, T., Dreis, S., Vogel, T., Gelperina, S., Langer, K., 2007. Covalent attachment of apolipoprotein A-I and apolipoprotein B-100 to albumin nanoparticles enables drug transport into the brain. J. Control. Release 118, 54–58.

Kreuter, J., Petrov, V.E., Kharkevich, D.A., Alyautdin, R.N., 1997. Influence of the type of surfactant on the analgesic effects induced by the peptide dalargin after its delivery across the blood–brain barrier using surfactant-coated nanoparticles. J. Control. Release 49, 81–87.

Kreuter, J., Shamenkov, D., Petrov, V., Ramge, P., Cychutek, K., Koch-Brandt, C., Alyautdin, R., 2002. Apolipoprotein-mediated transport of nanoparticle-bound drugs across the blood–brain barrier. J. Drug Target. 10, 317–325.

Li, R.T., Li, X.L., Xie, L., Ding, D., Hu, D., Qian, X.P., Yu, L.X., Ding, Y.T., Jiang, X.Q., Liu, B.R., 2009. Preparation and evaluation of PEG–PCL nanoparticles for local tetradrine delivery. Int. J. Pharm. 397, 158–166.

Liebmann, J., Cook, J.A., Lipschultz, C., Teague, D., Fishe, J., Mitchell, J.B., 1994. The influence of Cremophor EL on the cell cycle effects of paclitaxel (Taxol) in human tumor cell lines. Cancer Chemother. Pharmacol. 33, 331–339.

Liebmann, J., Cook, J.A., Mitchell, J.B., 1993. Cremophor EL solvent for paclitaxel and toxicity. Lancet 342, 1428.

Moore, A., Marcos, E., Bogdanov, A., Weissleder, R., 2000. Tumoral distribution of long-circulating dextran-coated iron oxide nanoparticles in a rodent model. Radiology 214, 568–574.

Mu, L., Feng, S.S., 2003. A novel controlled release formulation for the anticancer drug paclitaxel (Taxol): PLGA nanoparticles containing vitamin E TPGS. J. Control. Release 86, 33–48.

Olivier, J.C., Chauvet, R., Fenart, L., Pariat, C., Cecchelli, R., Couet, W., 1999. Nanoparticle technology for drug delivery across the blood–brain. Pharm. Res. 16, 1836–1842.

Ong, B.Y., Ranganath, S.H., Lee, L.Y., et al., 2009. Paclitaxel delivery from PLGA foams for controlled release in post-surgical chemotherapy against glioblastoma multiforme. Biomaterials 30, 3189–3196.

Owens III, D.E., Peppas, N.A., 2006. Opsonization, biodistribution, and pharmacokinetics of polymeric nanoparticles. Int. J. Pharm. 307, 93–102.

Pang, Z.Q., Lu, W., Gao, H.L., Hu, K.L., Chen, J., Zhang, C.L., Gao, X.L., Jiang, X.G., Zhu, C.Q., 2008. Preparation and brain delivery property of biodegradable polymersomes conjugated with OX26. J. Control. Release 128, 120–127.

Peracchia, M.T., Gref, R., Minamitake, Y., Domb, A., Lotan, N., Langer, R., 1997. PEG-coated nanospheres from amphiphilic diblock and multiblock copolymers: investigation of their drug encapsulation and release characteristics. J. Control. Release 46, 223–231.

Petri, B., Bootz, A., Khalansky, A., Hekmatara, T., Muller, R., Uhl, R., Kreuter, J., Gelperina, S., 2007. Chemotherapy of brain tumour using doxorubicin bound to surfactant-coated poly (butyl cyanoacrylate) nanoparticles: revisiting the role of surfactants. J. Control. Release 117, 51–58.

Pitt, C.G., 1990. Poly(ε-caprolactone) and its copolymers. In: Langer, R., Chasin, M. (Eds.), Biodegradable Polymers as Drug Delivery Systems. Marcel Decker Inc., New York, NY, pp. 71–120.

Postma, T.J., Heimans, J.J., Luykx, S.A., van Groeningen, C.J., Beenen, L.F., Hoekstra, O.S., Taphoorn, M.J., Zonnenberg, B.A., Klein, M., Vermorken, J.B., 2000. A phase II study of paclitaxel in chemonaive patients with recurrent high-grade. Ann. Oncol. 11, 409–413.

Ratner, B.D., Hoffman, A.S., Schoen, F.J., Lemons, J.E., 1996. Biomaterials Science. Academic Press, New York, pp. 347–356.

Régina, A., Demeule, M., Ché, C., 2008. Antitumor activity of ANG 1005, a conjugate between paclitaxel and the new brain delivery vector Angiopep-2. Br. J. Pharmacol. 155, 185–197.

Schiff, P., Fant, J., Horwitz, S.B., 1979. Promotion of microtubule assembly in vitro by Taxol. Nature 277, 665–667.

Shen, J., Zhan, C.Y., Xie, C., Meng, Q.G., Gu, B., Li, C., Zhang, Y.K., Lu, W.Y., 2010. Poly(ethylene glycol)-block-poly(D,L-lactide acid) micelles anchored with angiopep-2 for brain-targeting delivery. J. Drug Target. 6, 1–8.

Soo, P.L., Luo, L., Maysinger, D., Eisenberg, A., 2002. Incorporation and release of hydrophobic probes in biocompatible polycaprolactone-block-poly(ethylene oxide) micelles: implications for drug delivery. Langmuir 18, 9996–10004.

Steiniger, S.C.J., Kreuter, J., Khalansky, A.S., Skidan, I.N., Bobruskin, A.I., Smirnova, Z.S., Severin, S.E., Uhl, R., Kock, M., Geiger, K.D., Gelperina, S.E., 2004. Chemotherapy of glioblastoma in rats using doxorubicinloaded nanoparticles. Int. J. Cancer 109, 759–767.

Stewart, P.A., Hayakawa, K., Farrell, C.L., 1987. Quantitative study of microvessels ultrastructure in human peritumoral brain tissue. Evidence for a blood–brain barrier defect. J. Neurosurg. 67, 3293–3299.

Ten tije, A.J., Verweij, J., Loos, W.J., Sparreboom, A., 2003. Pharmacological effects of formulation vehicles: implication for canner chemotherapy. Clin. Pharmacokinet. 42, 665–685.

Walczyk, D., Bombelli, F.B., Monopoli, M.P., Lynch, I., Kenneth, A., Dawson, K.A., 2010. What the cell "sees" in bionanoscience. J. Am. Chem. Soc. 132, 5761–5768.

Wang, Y.Z., Li, Y.J., Han, L.M., Sha, X.Y., Fang, X.L., 2007. Difunctional Pluronic copolymer micelles for paclitaxel delivery: synergistic effect of folate-mediated targeting and Pluronic-mediated overcoming multidrug resistance in tumor cell lines. Int. J. Pharm. 337, 63–73.

Weiss, R.B., Donehower, R.C., Wiernik, P.H., 1990. Hypersensitivity reactions from Taxol. J. Clin. Oncol. 8, 1263–1268.

Zensi, A., Begley, D., Pontikis, C., Legros, C., Mihoreanu, L., Wagner, S., Büchel, C., Hagen von Briesen, H.V., Kreuter, J., 2009. Albumin nanoparticles targeted with Apo E enter the CNS by transcytosis and are delivered to neurons. J. Control. Release 137, 78–86.

Zhan, C.Y., Gu, B., Xie, C., Li, J., Liu, Y., Liu, W.Y., 2010. Cyclic RGD conjugated poly(ethylene glycol)-co-poly(lactic acid) micelle enhances paclitaxel anti-glioblastoma effect. J. Control. Release 143, 136–142.

Zhang, W., Hao, J.G., Shi, Y., Li, Y.J., Wu, J., Sha, X.Y., Fang, X.L., 2009. Paclitaxel-loaded Pluronic P123/F127 mixed polymeric micelles: formulation, optimization and in vitro characterization. Int. J. Pharm. 336, 176–185.

Zhang, W., Shi, Y., Chen, Y.Z., Yu, S.Y., Hao, J.G., Luo, J.Q., Sha, X.Y., Fang, X.L., 2010. Enhanced antitumor efficacy by Paclitaxel-loaded Pluronic P123/F127 mixed micelles against non-small cell lung cancer based on passive tumor targeting and modulation of drug resistance. Eur. J. Pharm. Biopharm. 75, 341–353.

Zhang, Z., Feng, S.S., 2006. The drug encapsulation efficiency, in vitro drug release, cellular uptake and cytotoxicity of Paclitaxel-loaded poly(lactide)-tocopheryl polyethylene glycol succinate nanoparticles. Biomaterials 27, 4025–4033.

Zhu, Z.S., Li, Y., Li, X.L., Li, R.T., Jia, Z.J., Liu, B.R., Guo, W.H., Wu, W., Jiang, X.Q., 2010. Paclitaxel-loaded poly(*N*-vinylpyrrolidone)-b-poly(ε-caprolactone) nanoparticles: preparation and antitumor activity in vivo. J. Control. Release 142, 438–446.